Astron. & Astrophys. 1, 270—280 (1969)

The Cygnus X Region

V. Catalogue and Distances of Optically Visible H II Regions

H. R. Dickel, H. Wendker*, and J. H. Bieritz
Vermilion River Observatory, USA

Received November 11, 1968

A catalogue of the H_α-emission nebulae in the western half of the Cygnus X region is presented. It contains positions, shapes and surface brightnesses in H_α of the nebulae. For 90 objects, which also have radio data, the distances are derived from reddening data. These distances range from 1 Kpc to greater than 4 Kpc. A ring of filaments surrounding the entire Cygnus X region is briefly discussed.

Key words: emission nebulae — stellar reddening — radio brightness — distance Cygnus X

1. Introduction

From analyses of optical and radio data, it appears that the emission nebulae which comprise the Cygnus X complex lie in a region of the local spiral arm which is viewed tangentially (e.g. Sharpless, 1965; Kerr and Westerhout, 1965). In Papers I and II of this series (Wendker, 1966 and 1967), the observational material was presented for the numerous radio sources which lie in the region between galactic longitudes 74° and 84° and between galactic latitudes $-2°$ and $+6°$. It was found that the emission from most of these sources is thermal and that the positions of the radio sources agree well with those of the optically visible H II regions.

The distances are not known for most of the objects. Ikhsanov (1960a and b), from a comparison of the H_α-emission and the radio emission from the brighter nebulae, and Véron (1965) from the assumption that the Cygnus II association is responsible for the excitation of the H II regions, both concluded that the distance to the complex is around 1500 pc. In Paper II several objections were raised against this idea that all the radio sources of the Cygnus X region are at one distance since the distances had been determined only for the few brightest H II regions. Therefore, it is important that the distances of all the nebulae be found.

One method for the determination of the nebular distances involves the finding of the distances to the known exciting stars. This method is difficult to use in the Cygnus X region because the exciting stars are generally not known and most of them would be inaccessible to observation due to heavy obscuration by the intervening interstellar dust. An alternative procedure involves a comparison of the observed radial velocities of the nebulae with those predicted from a model of galactic rotation. This procedure is also not applicable in the Cygnus X region because at this galactic longitude the radial velocity caused by galactic rotation changes only slowly with distance so that even a small peculiar motion makes an enormous difference in the derived distance. In view of these difficulties we are currently undertaking a program to determine the distances in another manner. We are comparing the H_α-surface brightnesses of the nebulae with their brightness temperatures at radio wavelengths (mainly at λ 11 cm). From this comparison we obtain a value for the interstellar absorption at λ 6563 ($= H_\alpha$) due to the intervening material. The dependence of the absorption upon distance can be derived from star-reddening data (see Ikhsanov, 1959b). The combination of these two data allows us to find the distance to each nebula.

For the above analysis, it was necessary to compile a new catalogue of nebulae for the Cygnus X region only, because the existing catalogues of H II regions are not suitably detailed and their intensity scales are not calibrated. The surface brightnesses tabulated in this new catalogue were estimated from calibrated plates of the H_α-emission in this region. The catalogue will also serve as a convenient reference for later papers of this series. In order to test the planned analysis it was applied to all nebulae in the catalogue for which radio brightness temperatures are available. The results from this

* Max Planck-Institut für Radioastronomie, Bonn, Germany.

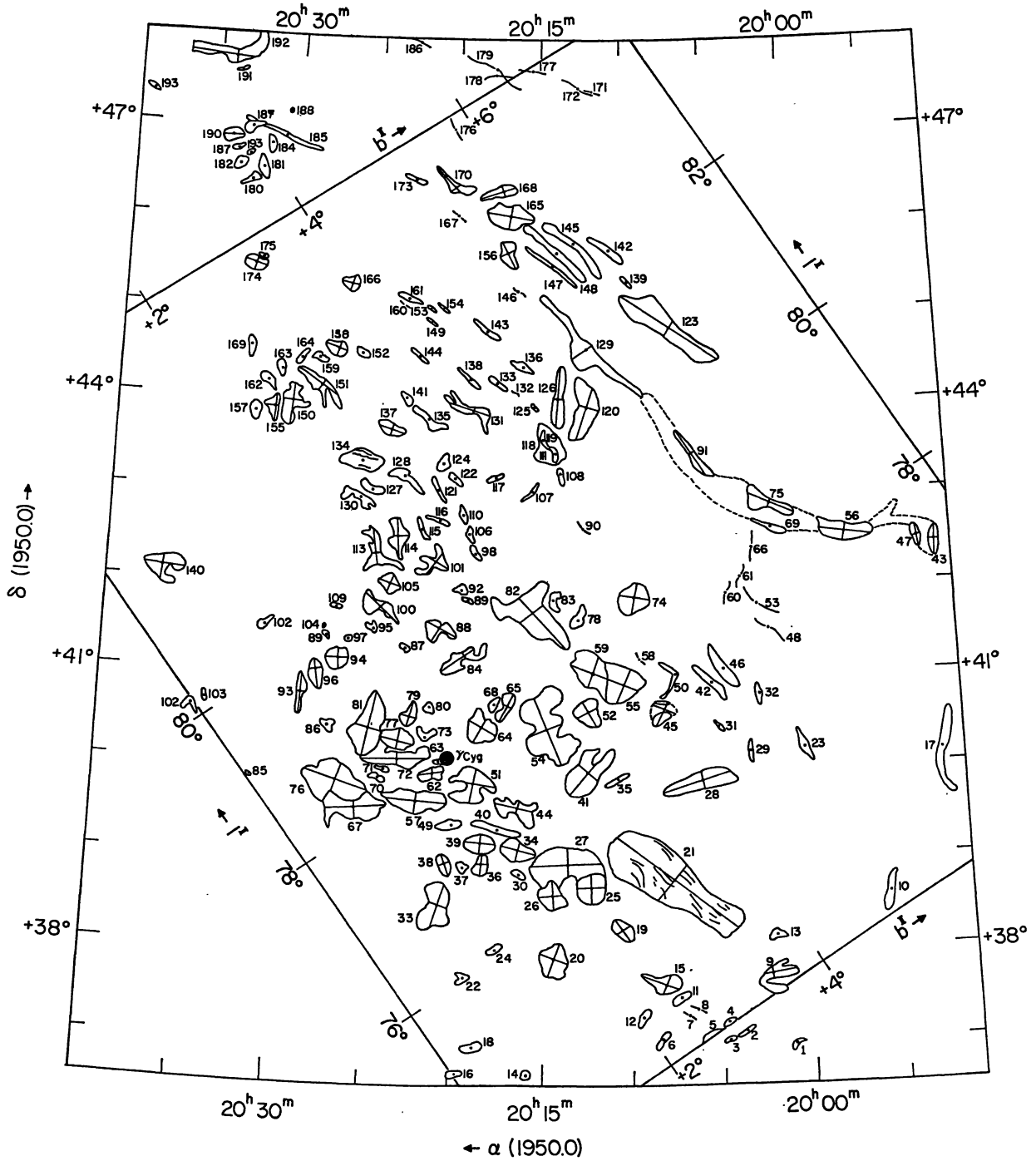

Fig. 1. Map of the H_α emission nebulae in the Cygnus X region. The numbers refer to the serial numbers in the Table (Erratum: There are two no. 193. The one near 187 should be 183.)

preliminary analysis indicate that a substantial number of the optically visible nebulae in Cygnus X are distributed along the line of sight instead of comprising a single collection at a distance of 1500 pc.

The purpose of this paper is twofold: 1. to present the catalogue of the H II regions in the Cygnus X complex and 2. to give preliminary estimates of their distances. The catalogue is presented in Section 2.

The numerical values used in the analysis are derived in Section 3 and the preliminary results are discussed in Section 4. A few comments concerning the ring of faint filaments surrounding the whole Cygnus X region are made in Section 5.

2. The Catalogue

a) The Preparation and Tabulated Results

The entire western half of the Cygnus X region is densely covered with nebulosities. In order to obtain a useful catalogue it was necessary to omit the faintest nebulae which form an apparent background. These undesired weak emissions were suppressed by laying semitransparent paper over the red prints of the National Geographic Society-Palomar Observatory Sky Survey. Then, only the outlines of the brighter nebulae were traced onto an α, δ coordinate grid. Several additional nebulae or substructures were found on plates taken with the 48-inch Schmidt telescope with an 80 Å wide interference filter centered on H_α (see section 2c). These nebulae were not seen on the Sky Survey because they were either over-exposed, blended with the image of a bright star such as γ Cygni, or their sharpness was impaired by the wider wavelength-band used in the Sky Survey. These extra features were added to the catalogue. Next, the position of the center of each nebulae was determined and for each one, two perpendicular axes — henceforth called major and minor axes — were drawn and measured. The resulting map is shown in Fig. 1. The numerical results are compiled in the Table.

b) Positions and Shapes

The serial number in column 1 of the Table was assigned only as an aid in the cross-reference of the Table and Fig. 1. To refer to individual nebulae we recommend and will use the G-number which indicates the galactic coordinates (see definition in Paper I or II). The position of the center of each nebulae was determined with regard to the outline of the nebula. In general, but not always, this position agrees with that of the brightest feature. Some of the axes were omitted in Fig. 1 whenever they would not be clearly visible.

For typical H II regions one expects the ratio of the lengths of the major and minor axes to be close to unity. However, many of the nebulae in the catalogue are not circular as can be seen from the histogram of the axis-ratios in Fig. 2. More than three-quarters of the nebulae have axis-ratios exceeding two. Two possible explanations for this anomalous behavior are: 1. the filamentary appearance of the nebulae is intrinsic, or 2. the appearance is merely a projection effect which is caused by the irregular pattern of the interstellar absorption (e.g. the dark lane between IC 1318b and c; = sources G 78.4 + 1.4, G 78.6 + 1.6, G 78.9 + 1.4 and G 78.3 + 0.8, G 78.6 + 0.7 in the catalogue). Very likely it is a combination of the two effects. We will return to this question in Section 5.

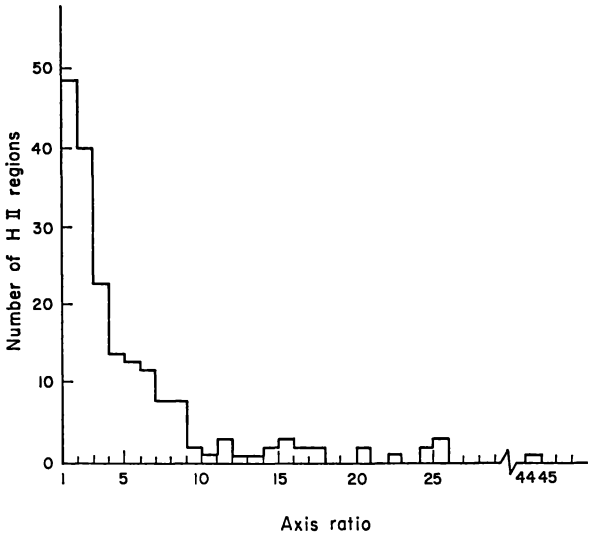

Fig. 2. Histogram of the number of nebulae per interval of axis-ratio

c) Calibration of Surface Brightnesses

In order to determine the surface brightnesses given in columns 8 and 9 of the Table, relative intensities were obtained from photographic plates which were exposed for 75 min through an 80 Å wide, H_α-interference filter on the 48-inch Schmidt telescope of the Mount Wilson and Palomar Observatories. The density of both the brightest emission and the average density within a circle of about 11′ diameter were estimated by eye by comparison with the density scale for the set of sensitometer spots which were on the plate. These surface brightnesses of the 11′ circle in column 9 are directly comparable to the emission measures in column 10. On the basis of a few measurements with the microphotometer it was found that the variation among plates is much less than the random errors for any one plate. The absolute calibration was obtained from photoelectric

Table. *Catalogue of the H_α-emission nebulae in the Cygnus X region*
(see end of Table for detailed explanation of the columns)

Number (1)	G — (2)	α (1950) (3)	δ (1950) (4)	Major axis (5)	Minor axis (6)	Galactic p. a. (7)	Surface brightness (8)	Surface brightness, (11′ beam) (9)	Radio emission measure (10)	Remarks (11)
1	G 73.4 + 3.3	20h01m.1	36°57′	6′.7	3′.3	168°				
2	G 73.8 + 2.9	03.7	37 05	13.3	3.2	178				
3	G 73.9 + 2.7	04.7	37 00	6.7	2.2	175				
4	G 74.0 + 2.8	04.7	37 11	8.9	2.2	177				
5	G 74.1 + 2.6	05.8	37 05	14.4	<1.0	174				
6	G 74.3 + 2.2	08.3	37 00	12.2	2.2	20				
7	G 74.3 + 2.5	06.9	37 15	7.8	<1.0	114				
8	G 74.3 + 2.6	06.4	37 20	10.0	<1.0	126				
9	G 74.3 + 3.4	02.3	37 42	21.6	7.8	154				Irregular
10	G 74.3 + 5.1	19 55.6	38 35	25.6	4.4	39				
11	G 74.5 + 2.5	20 07.2	37 28	13.3	4.4	0				
12	G 74.6 + 2.1	09.3	37 15	12.2	4.4	27				
13	G 74.6 + 3.8	01.9	38 10	8.9	5.6	132				
14	G 74.8 + 0.6	15.8	36 37	5.6	4.4	52				
15	G 74.8 + 2.5	08.1	37 37	26.6	13.3	121				
16	G 75.2 + 0.0	19.6	36 38	8.9	4.4	150				
17	G 75.3 + 6.4	19 52.2	40 07	41.1	5.6	41				
18	G 75.4 + 0.3	20 18.8	36 54	13.3	5.6	153				
19	G 75.5 + 2.4	10.5	38 12	16.7	11.1	89	>5.0	1.0		NGC 6888
20	G 75.6 + 1.6	14.3	37 52	23.3	18.9	36	0.2	0.1		
21	G 75.6 + 3.2	07.6	38 45	96.7	28.9	107	1.4	0.2		At least 42 filaments, wisps
22	G 76.0 + 0.7	19.2	37 41	5.6	5.6	145				
23	G 76.0 + 5.2	19 59.9	40 10	24.0	5.6	80				
24	G 76.1 + 1.1	20 17.5	37 58	8.9	4.4	169	0.2	0.05		
25	G 76.1 + 2.4	12.2	38 39	18.9	18.9	55	0.2	0.1	990	
26	G 76.2 + 2.0	14.3	38 35	20.0	15.6	59	0.2	0.1	1260	Rosette; many filaments on north
27	G 76.4 + 2.3	13.5	38 56	48.9	22.2	148	0.8	0.2	1480	Wisps
28	G 76.4 + 4.1	05.8	39 50	44.4	11.1	162	0.5	0.3		Knots
29	G 76.4 + 4.7	03.0	40 10	11.1	2.2	53	0.3	0.1		
30	G 76.7 + 1.8	16.3	38 50	8.9	4.4	122	0.5	0.2	2370	
31	G 76.7 + 4.5	04.8	40 26	8.9	1.1	100	0.4	0.1		
32	G 76.8 + 5.1	02.5	40 48	12.1	4.4	65				
33	G 76.9 + 0.9	20.7	38 30	30.0	12.2	38				
34	G 76.9 + 2.0	16.3	39 06	22.2	13.3	130	3.0	0.8	4000	
35	G 76.9 + 3.3	10.6	39 51	16.7	2.2	174	0.5	0.1	1650	
36	G 77.0 + 1.5	18.3	38 55	14.4	5.6	50	0.8	0.2	3340	
37	G 77.1 + 1.4	19.3	38 54	8.9	6.7	73	0.6	0.2	2410	
38	G 77.2 + 1.2	20.3	38 56	14.4	7.8	75				
39	G 77.2 + 1.7	18.4	39 09	20.0	12.2	142	1.2	0.3	4480	
40	G 77.2 + 1.9	17.5	39 19	32.2	4.4	130	2.4	0.8	5090	6 N-S filaments, "cold front"
41	G 77.2 + 3.1	12.3	39 57	25.6	15.6	15	3.0	0.5	2520	Includes 10 sharp filaments, blob of absorption at NW
42	G 77.2 + 4.7	05.1	40 55	27.8	3.3	100	0.5	0.2		
43	G 77.2 + 7.6	19 51.9	42 25	20.0	4.4	54				
44	G 77.3 + 2.2	20 16.3	39 33	24.4	7.8	133	1.0	0.3	4040	Many absorption lanes
45	G 77.3 + 4.1	08.0	40 38	17.8	16.7	32	0.5	0.2		
46	G 77.3 + 4.9	04.5	41 04	32.2	6.7	88	0.4	0.3		
47	G 77.3 + 7.5	19 52.9	42 28	15.6	4.4	64				
48	G 77.4 + 5.6	20 01.8	41 30	25.6	<1.0	114				
49	G 77.5 + 1.5	20.0	39 22	15.6	5.6	157	0.8	0.3	4200	6 sharp filaments
50	G 77.5 + 4.5	07.2	41 02	18.9	1.1	30	0.4	0.1		Boomerang
51	G 77.7 + 2.0	18.8	39 48	22.2	17.8	47	0.4	0.2	7270	*T*-shaped
52	G 77.7 + 3.4	12.3	40 36	18.9	16.7	86	1.2	0.5	3360	Elliptical

Table (continued)

Number (1)	G — (2)	α 1950) (3)	δ (1950) (4)	Major axis (5)	Minor axis (6)	Galactic p. a. (7)	Surface brightness (8)	Surface brightness, (11′ beam) (9)	Radio emission measure (10)	Remarks (11)
53	G 77.7 + 5.5	20h02m3	41°47′	25′.6	<1′.0	112°				
54	G 77.8 + 2.9	14.8	40 25	46.7	23.5	84	0.2	0.1	3330	Faint and patchy, irregular
55	G 77.8 + 3.9	10.5	40 55	25.6	21.2	125	1.2	0.6	1450	Sharp filaments
56	G 77.8 + 6.9	19 57.2	42 32	33.3	11.1	136				
57	G 77.9 + 1.4	20 22.0	39 37	37.8	14.4	140	*0.6*	*0.5*	5600	
58	G 77.9 + 4.2	09.3	41 11	6.7	<1.0	91	1.2	0.2	1260	
59	G 78.0 + 3.7	12.0	41 02	22.2	21.1	125	1.9	0.6	3310	Includes 3 long, bright streamers
60	G 78.0 + 5.4	04.2	41 55	14.4	<1.0	29				
61	G 78.0 + 5.6	03.3	42 05	16.7	<1.0	24				
62	G 78.1 + 1.7	21.2	39 55	16.7	6.7	153	0.6	0.2	20150	Faintly filamentary
63	G 78.2 + 1.8	20.8	40 03	5.6	3.3	148	3.0	0.8	24370	γ Cygni nebula
64	G 78.2 + 2.4	18.4	40 26	20.0	16.7	116	0.7	0.3	11150	Inverted horseshoe
65	G 78.2 + 2.8	16.9	40 40	20.0	5.6	31	1.9	0.8	7200	
66	G 78.2 + 5.9	02.6	42 24	20.0	<1.0	48				
67	G 78.3 + 0.8	25.5	39 32	38.9	11.0	150	*2.9*	*1.1*	6300	IC 1318c
68	G 78.3 + 2.6	17.7	40 40	8.9	5.6	28	0.5	0.1	11500	
69	G 78.3 + 6.2	01.5	42 37	23.3	3.3	126				
70	G 78.4 + 1.2	24.2	39 52	8.9	3.3	125	*1.0*	*0.6*	17280	
71	G 78.4 + 1.3	23.9	39 58	8.9	3.3	135	*1.0*	*0.8*	16300	
72	G 78.4 + 1.4	23.1	40 05	43.3	7.8	148	*2.4*	*1.0*	14300	SW part of IC 1318b
73	G 78.4 + 1.8	21.5	10 18	8.9	5.6	133	0.4	0.2	16120	
74	G 78.5 + 4.6	09.6	41 52	21.1	21.1	137	0.8	0.3	1320	Filamentary shell, brightest knot at NE
75	G 78.5 + 6.4	01.5	42 52	33.3	4.4	120				
76	G 78.6 + 0.7	26.8	39 49	43.3	18.9	129	*2.9*	*2.1*	14980	IC 1318c, hole near bottom
77	G 78.6 + 1.6	23.1	40 17	21.1	13.3	134	*1.7*	*1.0*	10700	NW part of IC 1318b, see G 78.4 + 1.4
78	G 78.6 + 3.9	12.9	41 38	16.7	6.7	26	0.2	0.1	2210	
79	G 78.7 + 1.8	22.5	40 32	17.8	10.0	40	*1.0*	*0.7*	6220	
80	G 78.7 + 2.0	21.4	40 38	6.7	6.7	124	0.2	0.1	7110	
81	G 78.9 + 1.4	24.7	40 25	43.3	17.8	45	*2.0*	*1.5*	10800	*E* part of IC 1318b, see G 78.4 + 1.4
82	G 78.9 + 3.6	15.5	41 42	45.6	20.0	98	4.6	3.0	8150	IC1318a, flares out at top
83	G 78.9 + 3.8	14.3	41 50	11.1	3.3	47	1.0	0.3	5560	
84	G 79.0 + 2.7	19.3	41 13	24.4	4.4	2	0.2	0.2	6000	Irregular
85	G 79.1 + 0.0	31.1	39 48	3.3	2.2	117				
86	G 79.2 + 1.0	27.3	40 26	10.0	5.6	104	*0.6*	*0.4*	4060	
87	G 79.4 + 2.2	22.8	41 18	7.8	3.3	111	0.4	0.1	11570	
88	G 79.4 + 2.6	20.9	41 30	21.1	12.2	116	0.3	0.2	8350	
89	G 79.4 + 3.1	19.2	41 50	6.7	2.2	133	0.6	0.3	4700	
90	G 79.4 + 4.5	12.6	42 38	11.1	<1.0	99	0.4	0.1	1060	
91	G 79.4 + 6.0	06.0	43 27	38.9	4.4	88				At least 4 filaments
92	G 79.6 + 3.1	19.2	41 57	7.8	5.6	138	0.3	0.2	4310	
93	G 79.7 + 1.0	28.8	40 48	28.9	4.4	54	0.2	0.1	7800	
94	G 79.9 + 1.5	26.7	41 10	14.4	14.4	56	1.1	0.4	4490	
95	G 79.7 + 2.0	24.6	41 29	7.8	4.4	113	0.5	0.2	3780	
96	G 79.8 + 1.3	28.0	41 02	20.0	7.8	62	0.4	0.1	8500	
97	G 79.8 + 1.7	26.1	41 22	4.4	2.2	135	0.4	0.1	6120	
98	G 79.8 + 3.4	18.8	42 21	10.0	3.3	82	0.9	0.2	3710	
99	G 79.9 + 1.7	27.3	41 25	6.7	2.2	102	0.3	0.1	9300	
100	G 79.9 + 2.2	24.3	41 45	28.9	11.0	106	1.0	0.3	6220	
101	G 80.0 + 3.0	21.0	42 15	17.8	12.2	22	0.5	0.2	3520	
102	G 80.1 − 0.0	34.6	40 36	6.7	6.7	135				
103	G 80.1 + 0.1	33.9	40 40	6.7	2.2	62				

Table (continued)

Number (1)	G — (2)	α (1950) (3)	δ (1950) (4)	Major axis (5)	Minor axis (6)	Galactic p. a. (7)	Surface brightness (8)	Surface brightness, (11′ beam) (9)	Radio emission measure (10)	Remarks (11)
104	G 80.1 + 1.6	$20^h27^m.6$	41°30′	2′.2	1′.1	38°	0.3	0.1	10300	
105	G 80.1 + 2.5	23.8	42 01	14.4	11.1	124	1.2	0.4	5520	
106	G 80.1 + 3.5	19.2	42 35	10.0	4.4	55	0.3	0.1	3130	
107	G 80.1 + 4.3	15.5	43 02	16.7	1.1	13	1.5	0.2	1770	
108	G 80.1 + 4.7	13.9	43 14	11.1	2.2	61	0.3	0.2	1020	
109	G 80.2 + 1.8	26.9	41 43	7.8	2.2	140	0.3	0.1	4720	
110	G 80.3 + 3.5	19.6	42 46	11.1	4.4	68	0.3	0.2	3000	
111	G 80.3 + 4.8	14.3	43 31	11.1	2.2	101	3.0	~ 1.5	3200	SW part of Hase and Shajn (1955) No. 191
112	G 80.4 + 1.1	30.8	41 30	13.3	5.6	3	1.2	0.2	~ 6400	
113	G 80.4 + 2.5	24.6	42 20	24.4	5.6	64	0.3	0.2	2740	*L*-shaped
114	G 80.4 + 2.8	23.3	42 31	25.6	5.6	59	0.8	0.3	4200	
115	G 80.4 + 3.1	21.9	42 37	14.4	1.1	72	0.5	0.1	4650	
116	G 80.4 + 3.3	21.0	42 42	16.7	1.1	128	0.6	0.1	3600	
117	G 80.4 + 4.0	17.7	43 10	12.2	2.2	168	0.4	0.1	2330	
118	G 80.4 + 4.7	14.7	43 31	23.3	22.0	76	1.1	~ 1.5	3200	SW part of HS 191, see G 80.3 + 4.8
119	G 80.5 + 4.7	14.9	43 37	11.1	2.2	86	2.4	~ 1.5	3200	NE part of HS 191, see G 80.3 + 4.8
120	G 80.5 + 5.3	12.3	43 57	37.8	12.2	40	0.1	0.1	1410	
121	G 80.6 + 3.5	21.0	43 02	16.7	2.2	81	0.6	0.1	3330	
122	G 80.6 + 3.7	20.0	43 10	12.2	2.2	103	0.2	0.1	2420	
123	G 80.7 + 6.5	07.2	44 50	74.4	12.2	111	0.2	0.1		
124	G 80.8 + 3.7	20.8	43 20	13.3	7.8	24	0.3	0.1	1810	
125	G 80.0 + 4.8	15.5	43 58	5.6	1.1	92	1.0	0.3	1770	
126	G 80.8 + 5.1	14.1	44 03	37.8	5.6	51	0.3	0.1	2640	
127	G 80.9 + 3.2	23.0	43 10	23.3	5.6	102	1.2	0.3	3410	
128	G 81.0 + 2.9	24.9	43 01	15.6	3.3	120	1.2	0.3	3140	
129	G 81.0 + 5.7	12.3	44 36	93.3	15.6	100				Bulge in middle
130	G 81.1 + 2.7	25.7	42 57	22.2	3.3	118	0.8	0.3	2740	
131	G 81.1 + 4.3	19.0	43 55	30.0	4.4	126	1.2	0.5	1720	Notch on top
132	G 81.1 + 4.7	16.6	44 07	5.6	< 1.0	118	0.2	0.1	1460	
133	G 81.2 + 4.6	17.7	44 12	14.3	2.2	108	0.5	0.3	1630	
134	G 81.3 + 3.0	25.5	43 20	27.8	13.3	139	0.5	0.1	4360	2 parallel filaments
135	G 81.3 + 3.8	21.8	43 48	22.2	3.3	103	1.2	0.3	2540	Tilted *L*
136	G 81.3 + 5.0	16.1	44 25	15.5	5.6	121	1.2	0.4		
137	G 81.4 + 3.4	23.8	43 41	16.7	7.8	128	0.3	0.1	3080	
138	G 81.4 + 4.4	19.2	44 15	18.9	2.2	102	0.3	0.1	1420	
139	G 81.4 + 6.4	09.8	45 20	10.0	2.2	91				
140	G 81.5 + 0.8	35.6	42 07	26.7	15.5	141	0.2	0.1	10200	Horseshoe, contains DR 21
141	G 81.6 + 3.8	22.9	44 02	8.9	4.4	88	0.3	0.1	2110	
142	G 81.7 + 6.4	10.9	45 31	27.8	4.4	107	0.05	0.05		
143	G 81.8 + 4.9	18.3	44 47	20.0	2.2	103	1.2	0.5		
144	G 81.9 + 4.1	22.2	44 30	15.6	2.2	102	0.2	0.1		
145	G 81.9 + 6.1	13.1	45 35	50.0	4.4	104	0.3	0.1		At least 7 faint wisps
146	G 82.0 + 5.4	16.3	45 15	8.9	< 1.0	117	0.4	—		
147	G 82.0 + 5.9	14.4	45 31	44.4	2.2	106	0.3	0.05		
148	G 82.1 + 6.0	14.1	45 39	53.5	4.4	103	1.0	0.2		
149	G 82.2 + 4.6	21.5	44 52	8.9	1.1	107				
150	G 82.3 + 2.7	29.8	43 58	27.8	12.2	51	0.8	0.2	7620	
151	G 82.3 + 3.1	28.2	44 10	28.9	7.8	112	0.8	0.2	3360	Fork-shaped
152	G 82.3 + 3.6	25.7	44 31	10.0	4.4	117	0.1	0.05		
153	G 82.3 + 4.5	21.7	45 02	6.7	1.1	116				
154	G 82.3 + 4.6	20.9	45 03	10.0	1.1	112				
155	G 82.4 + 2.5	30.8	43 54	17.8	8.9	52	0.4	0.1	9280	
156	G 82.4 + 5.5	17.1	45 38	18.9	11.1	81	1.2	0.1		Hole in middle

Table (continued)

Number (1)	G — (2)	α (1950) (3)	δ (1950) (4)	Major axis (5)	Minor axis (6)	Galactic p. a. (7)	Surface brightness (8)	Surface brightness, (11′ beam) (9)	Radio emission measure (10)	Remarks (11)
157	G 82.5 + 2.3	20h32m.0	43°51′	13′.3	7′.8	60°	0.3	0.1	9680	
158	G 82.5 + 3.2	28.4	44 27	11.1	4.4	112	0.3	0.1		
159	G 82.5 + 3.5	27.2	44 34	14.4	10.0	127	0.1	0.1		
160	G 82.5 + 4.3	23.2	45 05	8.9	1.1	107				
161	G 82.5 + 4.4	22.9	45 08	17.8	3.3	122				
162	G 82.7 + 2.7	31.2	44 12	14.4	4.4	85	0.3	0.1	4740	
163	G 82.7 + 2.8	30.5	44 19	10.0	5.6	59	0.1	0.05	3150	
164	G 82.7 + 3.1	29.3	44 27	11.1	3.3	27	0.5	0.1		
165	G 82.7 + 5.8	16.9	46 03	31.1	14.4	135	1.0	0.5		
166	G 83.0 + 4.0	26.5	45 17	11.1	10.0	131				
167	G 83.0 + 5.3	20.1	46 04	11.1	<1.0	109	0.6	0.2		
168	G 83.0 + 5.9	17.5	46 20	24.4	6.7	162	0.2	0.05		
169	G 83.1 + 2.7	32.4	44 35	13.3	5.6	56	0.2	0.1		
170	G 83.3 + 5.5	20.3	46 22	23.3	6.7	99	0.4	0.1		Tilted *L*, 7 small wisps
171	G 83.4 + 7.3	11.8	47 25	11.1	<1.0	131				
172	G 83.5 + 7.2	12.8	47 27	24.4	<1.0	117				
173	G 83.6 + 5.2	22.7	46 27	15.6	2.2	123				
174	G 83.8 + 3.3	32.3	45 28	14.4	7.8	125				
175	G 83.8 + 3.4	31.9	45 32	5.6	2.2	131				
176	G 83.8 + 5.8	20.3	47 00	16.7	<1.0	81				
177	G 83.9 + 6.9	15.5	47 39	17.8	<1.0	140				
178	G 84.1 + 6.5	17.8	47 35	20.0	<1.0	145				
179	G 84.4 + 6.8	17.8	48 00	44.4	<1.0	115				
180	G 84.6 + 3.7	32.7	46 22	15.6	3.3	168				
181	G 84.6 + 3.9	32.2	46 32	16.7	6.7	68				
182	G 84.8 + 3.7	33.5	46 33	10.0	7.8	176				
183	G 84.8 + 3.9	33.0	46 40	5.6	3.3	168				
184	G 84.8 + 4.2	31.7	46 48	11.1	3.3	62				
185	G 84.8 + 4.3	30.8	46 54	55.6	2.2	125				Partly behind (?) G 85.0 + 4.1
186	G 84.8 + 6.1	22.6	47 58	15.6	<1.0	115				
187	G 84.9 + 3.8	33.7	46 43	7.3	2.2	151				
188	G 84.9 + 4.6	30.6	47 10	3.3	2.2	90				
189	G 85.0 + 4.1	32.9	46 58	13.3	7.8	147				
190	G 85.1 + 3.8	34.3	46 51	13.3	7.8	145				
191	G 85.6 + 4.3	33.8	47 33	7.8	2.2	166				
192	G 85.8 + 4.4	34.2	47 44	41.1	8.9	140				Only partly on map
193	G 86.0 + 3.5	39.2	47 18	8.9	1.1	113				

Explanation of columns:

1. a serial number,
2. the *G* number of the center (see section 2b),
3. and 4. the right ascension and declination of the center (1950.0),
5. and 6. the lengths (in minutes of arc) of the major and minor axes,
7. the position angle of the major axis measured eastward (counter clockwise) from galactic north,
8. the surface brightness in H_α (in 10^{-4} ergs cm^{-2} s^{-1} $ster^{-1}$) for the most intense emission,
9. the same surface brightness as would be measured with a resolution of 11′,
10. the radio emission measure (as used in section III, from Wendker, 1968),
11. remarks on the shape, etc.

measurements of the 4 brightest nebulae (G 78.9 + 1.4, G 78.6 + 0.7, G 78.9 + 3.6, and G 80.3 + 4.8) with a spectral scanner attached to the 24-inch Morgan telescope of the Lowell Observatory. The details of both the photographic and photoelectric observations will be presented in a later paper.

As the plates were taken with an 80 Å wide filter, the relative intensities include both the emission from H_α at 6563 Å and from the nearby forbidden nebular lines of nitrogen [N II] at 6548 and 6584 Å. However, from photoelectric measurements of 11 nebulae, we found that the ratio of intensities, $I_{[N\,II]}/I_{H_\alpha}$, is essentially constant with a value near 0.5. Thus the scale of the sensitometer spots could be directly converted into the intensity scale for H_α alone without introducing significant errors. So far, isophotes have been made for only one plate. These isophotes were calibrated with the photoelectric data. Thus it was possible to determine very accurate surface brightnesses for the nebulae which were on this first plate. These surface brightnesses are in italics in column 8. From a comparison of the estimated surface brightnesses with the accurately measured values for these nebulae we find that there may be a trend toward slightly over-estimating the surface brightness of the bright objects and underestimating the brightness of the faint ones.

3. The Method of Analysis

For any nebula, the observed surface brightness in H_α, S_{H_α}, and the observed radio brightness temperature, T_b, are directly related to the emission measure (see Eqs. (2) and (4) below). Thus, if there is no absorption of the optical radiation by interstellar material, then one should obtain identical values for the emission measure at both wavelengths. If, however, absorption does occur, then the ratio of the emission measure found from the radio observations, E_{rad}, to that from the H_α observations, E_{H_α}, is the amount of the total absorption in H_α (i.e. A_{H_α}, if the absorption is expressed in magnitudes). From the measured color-excesses of stars in the same direction, one can obtain the dependence of the absorption upon the distance (see Section 3e). The formulae and numerical values which are required in the above analysis are summarized in the following sections *a* through *e*.

a) Choice of the Electron Temperature, T_e

Many of the parameters in these calculations depend upon the electron temperature, T_e, of the nebula. The nebulae are too faint for one to obtain the usual measurements for the determination of T_e directly. Furthermore, the derived T_e is sensitive to the type of observations used; the extreme range of the measured T_e's for various H II regions is from 3000° to 10000 °K (e.g. Peimbert, 1967; Mezger and Höglund, 1967). We shall therefore adopt the average value of $T_e = 6000$ °K in our calculations and we will discuss the dependence of each parameter upon T_e.

b) Conversion of S_{H_α} into E_{H_α}

The relationship between S_{H_α} and E_{H_α} is

$$S_{H_\alpha} = a_{H_\alpha} \cdot E_{H_\alpha}, \tag{1}$$

where the coefficient a_{H_α} is evaluated for case *B* from the paper by Pengelly (1964). For $T_e = 6000$ °K, it follows that

$$E_{H_\alpha}[\mathrm{cm^{-6}\ pc}] = 710 \cdot S_{H_\alpha}[10^{-4}\ \mathrm{cgs\ units}]. \tag{2}$$

The factor of proportionality is a function of T_e; for $T_e = 7500$ °K, it would be 870 instead of 710.

c) Conversion of T_b into E_{rad}

For an optically thin nebula, the expression relating T_b and E_{rad} is

$$T_b = a_{rad} \cdot E_{rad} \cdot T_e, \tag{3}$$

where a_{rad} is a function of the frequency, ν, and of T_e. It may be calculated from Eq. 151 in Oster, 1961. For a frequency of 2695 MHz (used by Wendker, 1968) and for $T_e = 6000$ °K,

$$E_{rad}[\mathrm{cm^{-6}\ pc}] = 2060 \cdot T_b[\mathrm{°K}]. \tag{4}$$

For $T_e = 7500$ °K, the factor of proportionality becomes 2210.

d) The Total Absorption, A_{H_α}

The total absorption, A_{H_α}, is determined from the ratio of the emission measures:

$$A_{H_\alpha}[\mathrm{mag.}] = 2.5 \cdot \log\left(\frac{E_{rad}}{E_{H_\alpha}}\right). \tag{5}$$

Using Eqs. (2) and (4) we may rewrite Eq. (5) as

$$\begin{aligned} A_{H_\alpha} &= 2.5 \cdot \log\left(\frac{2.9 \cdot T_b}{S_{H_\alpha}}\right) \\ &= 1.156 + 2.5 \cdot \log\left(\frac{T_b}{S_{H_\alpha}}\right). \end{aligned} \tag{6}$$

If T_e is raised from 6000° to 7500 °K, then the total absorption decreases by about 0.15 mag.

The absorption is often given in terms of that in the visual, A_V. Since it is A_V which is available from the star-reddening data, we convert the values of A_{H_α} into A_V via the reddening curve by Whitford (1958):

$$A_V = 1.28 \cdot A_{H_\alpha}. \tag{7}$$

e) A_V as a Function of Distance

The total A_V of the stellar radiation by the interstellar dust is related to the measured color-excess $\mathscr{E}_{B-V}$ by the expression

$$A_V = R \cdot \mathscr{E}_{B-V}, \quad (8)$$

where the ratio, R, of total to selective absorption is assumed equal to 3. Recently, there has been considerable controversy over the actual value of R (Johnson, 1968). However, we feel justified in using $R = 3$ for two reasons: most observers seem to agree that for the Cygnus X region the value is close to 3 (Johnson, 1968), and from a study of many H II regions, Gebel (1968) found that the value of R is also close to 3 for nebular radiation.

The distance to the star is then determined from a comparison of the absolute and apparent magnitudes of the star [after the latter is corrected for interstellar absorption by Eq. (8)]. From these stellar data for a given area in the sky one can plot the absorption as a function of distance. To obtain a well-defined curve, one needs many stars down to as faint a magnitude as possible. We find that the survey by Ikhsanov (1959a, b) contains the most extensive and consistent set of data available for this particular region where we have both the radio and H_α data. Ikhsanov divided the area into 8 subsections and derived the absorption as a function of distance for each. Although it is known that the pattern of absorption can be very irregular, we have used a single curve for each of his subsections because to further subdivide the region would drastically reduce the number of stars available for each curve.

Ikhsanov's curve 7 is poorly defined. The absorption is flat until 1.5 Kpc, and then rises steeply. However, he gives no stellar data for distances greater than 1.8 Kpc. For region 7 we used curve 4 because its shape is the closest to that indicated by an extrapolation of curve 7. The distances may be underestimated for about 12 of the objects in region 7.

4. Preliminary Results

a) The Distances

We have applied the analysis as outlined in Section 3 to 90 nebulae for which the values of S_{H_α} and T_b are available. In Fig. 3 we summarize the results in the form of a histogram of the number of nebulae per interval of distance from the sun. We see that less than half of the nebulae are between the distances of 1.2 and 1.8 Kpc. There are no nebulae closer than 1 Kpc. The number of objects per distance interval decreases gradually out to 3.6 Kpc. About one-fifth of the sources lie at

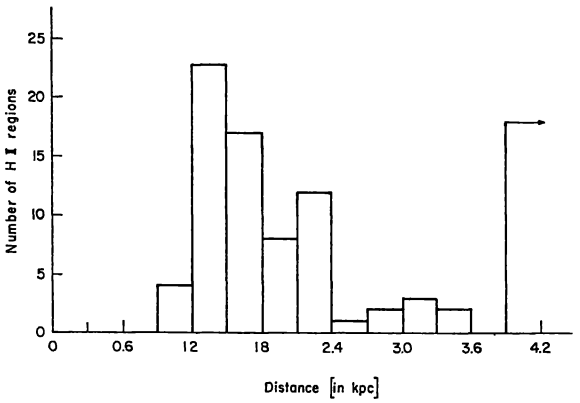

Fig. 3. Histogram of the number of nebulae per interval of distance

distances greater than 4 Kpc. At the present time there are no data available for stars at distances greater than 4 Kpc. Thus the distances to these nebulae can not be determined. The histogram clearly shows that the nebulae in the Cygnus X region are not all grouped at one distance but are spread out along the spiral arm in the line of sight. It is not possible to determine the significance of the apparent gap just before 4 Kpc. We also do not know the spatial relationship of the nebulae beyond 4 Kpc with respect to the rest of the nebulae, i.e. into which spiral arm they belong. (See also the discussion of possible errors in Section 4b, 1.) To obtain more definitive results we need stellar data to fainter magnitudes. From an examination of Ikhsanov's absorption-curves, one might expect an additional absorption of $\leqq 2$ magnitudes from 4 Kpc to 6 Kpc. Thus, if data were available for O and B stars up to apparent magnitude 16, then the curves of absorption vs. distance could be extended to 6 Kpc and some of the uncertainties in the nebular distances could be removed.

b) Discussion of the Assumptions

The nebulae selected for the catalogue are those which are optically visible and brighter than a certain limit (see Section 2a). Thus the sample is biased toward those which either are intrinsically the brightest or are the least affected by absorption. The fainter nebulae will be included in the future,

after all of the plates have been calibrated in surface brightness units. Furthermore, because of observational limitations, only the western half of the Cygnus X region was analyzed; the results do not necessarily apply to the other half.

There are five observational factors which can introduce systematic errors into the values found for the distances. Four of these are related to the total absorptions derived for the nebulae. The fifth is concerned with the curves of absorption vs. distance which were derived from the stellar data. 1. If, as mentioned at the end of Section 2c, the surface brightnesses of the faintest nebulae should be underestimated by a factor of 2, then the nebulae that were found to be greater than 4 Kpc away would actually be just under 4 Kpc. The nearer nebulae would be less affected. These possible discrepancies will be removed when the detailed analysis is completed. 2. Our value adopted for the ratio $I_{[\mathrm{N\,II}]}/I_{\mathrm{H}_\alpha}$ is very close to that found by other observers (e.g. Johnson, 1953). Our observed scatter in this ratio would introduce a random error of less than 0.1 Kpc in the derived distance. 3. Even with a resolution of 11′ there is not a clear separation of the radio sources from one another and an unresolved background component of the emission may be present. In Paper I it was shown that the background at this frequency of 2695 MHz is very likely to be of thermal origin and may be due merely to unresolved nebular radiation. Therefore, for the present analysis we used the observed values of the brightness temperature and did not remove any background component. If one were to subtract a background component from the data, then the calculated distances would be less than the ones obtained here. (For a more complete discussion of this point, see the paper by Wendker, 1968.) 4. As pointed out in Section 3d, an increase in the adopted electron temperature by 1500 °K would decrease the absorption by less than 0.2 mag. and thus decrease the distance by about 0.2 Kpc. The relative distances are changed only when there is a variation in T_e among the nebulae. 5. The choice of R can also cause a possible systematic error in the derived distances. If R is greater than the assumed value of 3 (see Section 3e), then the plots of absorption vs. distance would be altered and the distances to the nebulae would be lower. Furthermore, one should keep in mind that each such plot given by Ikhsanov applies to a large area. If the absorption is very irregular, then this patchiness would act as a random error in the derived nebular distances.

In summary, we think that the differences in the amount of absorption for different nebulae are reasonably well determined but that the actual distances may be systematically biased. We estimate the mean random errors to be of the order of 25 to 30 percent.

c) The Nearby Nebulae

It is interesting to note that the optically bright nebulae IC 1318a, b, c and Hase and Shajn No. 191 (these include our catalogue sources G 78.9 + 3.6; G 78.4 + 1.4, G 78.6 + 1.6, G 78.9 + 1.4; G 78.3 + 0.8, G 78.6 + 0.7; and G 80.3 + 4.8, G 80.4 + 4.7, G 80.5 + 4.7) are also among the closest. The determination of the distances to the Cygnus X complex in earlier studies (Ikhsanov, 1960b; Véron, 1965) was greatly influenced by these nebulae. Their distances do, on the average, lie near 1.5 Kpc. The so-called γ Cygni nebula, G 78.2 + 1.8, seems to belong to this group also. On the Sky Survey prints it is hidden by the over-exposed image of the star γ Cygni, but on the H_α plates it is quite clearly separated. The nebulosity appears fairly bright with a diameter of about 3′. The γ Cygni radio source has a strong non-thermal component (Paper I and Higgs and Halperin, 1968) but, using the 150-foot telescope at a frequency of 10.63 GHz, Higgs and Halperin were able to resolve a small thermal source from the wider non-thermal one. There is excellent agreement in the positions of this small source and the H_α emission nebulae (see Plate I of their paper). Therefore, we may obtain a distance for the nebula. From Fig. 2 of Higgs and Halperin, the brightness temperature T_b at 10.63 GHz is estimated to be about 0.48 °K and from the plates the surface brightness in H_α is about 3.0 ($\times 10^{-4}$ cgs). This leads to an absorption of $A_V = 2.8$ mag. or a distance of about 1.2 Kpc. Thus it appears that the confusion which has existed over the γ Cygni nebula is caused by a projection onto the same line of sight of the star γ Cygni (at a distance of about 215 pc according to Higgs and Halperin, 1968), the H_α emission nebula (at about 1.2 Kpc) and the non-thermal radio component (at about 3 Kpc according to Higgs and Halperin, 1968).

5. The Ring of Filaments

A ring of filaments which appears to enclose the whole Cygnus X region is mentioned in the papers by Morgan, Strömgren and Johnson (1955); Struve (1957) and Ikhsanov (1960b). This ring structure is most pronounced in the west and southeast. A sketch

of all the elongated filaments which seem to belong to this ring is shown in Fig. 4. The ring is well defined except for a few gaps at small galactic latitudes. The surface brightness of these filaments in H_α is quite low. Their typical emission measures E_{H_α} are about $100\,(cm^{-6}\,pc)$ or less. Radio data are almost non-existent. Ikhsanov (1960b) concluded that this ring forms the outer boundary of the single nebular complex which is excited by the Cygnus II association. It follows from our analysis that the Cygnus II association cannot be responsible for the excitation of all these nebulae. Therefore, for the moment we will refrain from making any definite statement with regard to the location or origin of the ring.

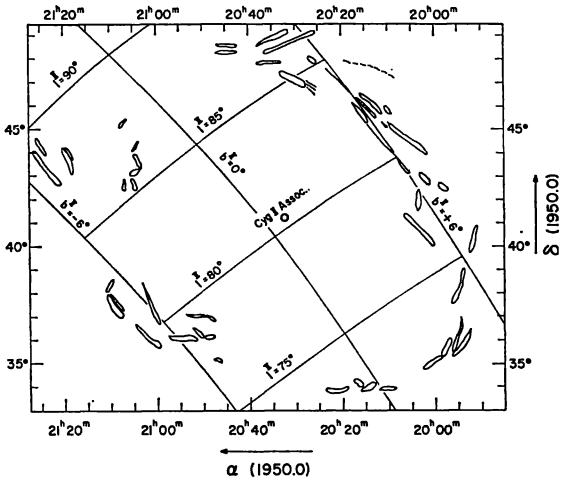

Fig. 4. The ring of filaments around the Cygnus X region

6. Summary

We have presented a catalogue and a map of the H II regions in the western half of the Cygnus X region for use as a general reference. From a preliminary analysis of the observational material we have concluded that the nebulae have distances ranging from 1 to greater than 4 Kpc. The socalled γ Cygni nebula is not intrinsically associated with the star γ Cygni. This nebula belongs to a group of the brightest nebulae which lie nearby at a distance of about 1.5 Kpc.

The details of this investigation are being refined in the accurately calibrated analysis which is currently in progress. This analysis will require a long time to complete (especially the microphotometry of all the plates). However, we expect the overall picture to remain unchanged. This refined analysis will yield H_α contour maps with 1′ resolution which can later be convolved to any resolution required by the radio data. Then a distance can be calculated for each point in the grid. The greatest problem may well be the scarcity of star-reddening data.

Acknowledgement. We wish to thank Prof. G. C. McVittie for his continuous encouragement and support of this study. We would like to thank Dr. J. S. Hall, Director of the Lowell Observatory and Dr. H. W. Babcock, Director of the Mt. Wilson and Palomar Observatories for the generous amount of observing time allocated to us. We appreciated the able and kind help that the staff of both observatories gave us with the equipment and observations. We are grateful to Drs. J. R. Dickel, J. Cahn and J. B. Kaler for reading the manuscript.

This research has been partially supported by the Office of Naval Research under Contract Nonr NO014 and by the National Science Foundation under Grant GP-6576.

References

Gebel, W. 1968, Ap. J. **153**, 743.
Hase, V. F. and Shajn, G. A. 1955, Izv. Krymsk. Astrofiz. Observ. **15**, 11.
Higgs, L. A. and Halperin, W. 1968, Mon. Not. Roy. Astr. Soc. **141**, 209.
Ikhsanov, R. N. 1959a, Izv. Krymsk. Astrofiz. Observ. **21**, 229.
Ikhsanov, R. N. 1959b, Izv. Krymsk, Astrofiz. Observ. **21**, 257.
Ikhsanov, R. N. 1960a, Izv. Krymsk. Astrofiz. Observ. **23**, 31.
Ikhsanov, R. N. 1960b, Astr. Zhurnal. **37**, 988.
Johnson, H. L. 1968, in Nebulae and Interstellar matter, ed. B. M. Middlehurst and L. H. Aller. Chicago, Univers. of Chica. Press. 167.
Johnson, H. M. 1953, Ap. J. **118**, 370.
Kerr, F. J. and Westerhout, G. 1965, in Galactic Structure, ed. A. Blaauw and M. Schmidt. Chicago, Univers. of Chica. Press. 167.
Mezger, P. G. and Höglund, B. 1967, Ap. J. **147**, 490.
Morgan, W. W., Strömgren, B. and Johnson, H. M. 1955, Ap. J. **121**, 611.
Oster, L. 1961, Rev. Mod. Phys. **33**, 525.
Peimbert, M. 1967, Ap. J. **150**, 825.
Pengelly, R. M. 1964, Mon. Not. Roy. Astr. Soc. **127**, 145.
Sharpless, S. 1965, in Galactic Structure, ed. A. Blaauw and M. Schmidt, Chigaco, Univers. of Chica. Press. 131.
Struve, O. 1957, Sky and Telescope **16**, 118.
Véron, P. 1965, Ann. Astr. **28**, 391.
Wendker, H. 1966, Mitt. Astr. Inst. Münster No. 10 Paper I.
Wendker, H. 1967, Z. Astrophys. **66**, 379, Paper II.
Wendker, H. 1968, in preparation.
Whitford, A. E. 1958, Astron. J. **63**, 201.

Hélène R. Dickel
Heinrich Wendker*
John H. Bieritz
Vermilion River Observatory
University of Illinois
Urbana, Illinois, USA

* present address:
Max-Planck-Institut für Radioastronomie
5300 Bonn, Argelanderstraße 3, Germany